

- 1) Running title: Isorhamnetin activates lysosomes in J774.1 macrophages.
- 2) title: Isorhamnetin, a 3'-methoxylated flavonol, enhances the lysosomal proteolysis in J774.1 murine macrophages in a TFEB-independent manner.
- 3) Maiko SAKAI¹, Kohta OHNISHI*¹, Masashi MASUDA¹, Hirokazu OHMINAMI¹, Hisami YAMANAKA-OKUMURA¹, Taichi HARA², Yutaka TAKETANI*¹
- 4) 1. Department of Clinical Nutrition and Food Management, Institute of Biomedical Sciences, Tokushima University Graduate School, Tokushima, 770-8503, Japan
2. Laboratory of Food and Life Science, Faculty of Human Sciences, Waseda University, Saitama, 359-1192, Japan.
- 5) *To whom correspondences should be addressed.
Tel: +81-88-633-9595; Fax: +81-88-633-7094; E-mail: ohnishi.kohta@tokushima-u.ac.jp (K. OHNISHI) & taketani@tokushima-u.ac.jp (Y. TAKETANI)
- 6) Abbreviations:
ANOVA, analysis of variance; ApoE, apolipoprotein E; ATP6V0D2, ATPase H⁺ transporting V0 subunit d2; BAF, bafilomycin A1; BODIPY, boron dipyrromethene; BSA, bovine serum albumin; CTSD, cathepsin D; CTSF, cathepsin F; DMEM, Dulbecco's modified eagle medium; DMSO, dimethyl sulfoxide; EGCG, epigallocatechin-3-gallate; FBS, fetal bovine serum; GAPDH, glyceraldehyde-3-phosphate dehydrogenase; HPLC, high-performance liquid chromatography; LAMP1, lysosomal-associated membrane protein 1; LAMP2A, lysosomal-associated membrane protein 2A; LC-MS/MS, liquid chromatography tandem mass spectrometry; MITF, microphthalmia-associated transcription factor; MRM, multiple reaction monitoring; mTORC1, mechanistic target of rapamycin complex 1; PBS, phosphate-buffered saline; PPAR γ , peroxisome

24 proliferator-activated receptor γ ; RT-qPCR, reverse transcription quantitative polymerase
25 chain reaction; SDS, sodium dodecyl sulfate; SNARE, soluble N-ethylmaleimide-
26 sensitive-factor attachment protein receptor; TBS, Tris-buffered saline; TFA,
27 trifluoroacetic acid; TFE3, transcription factor binding to IGHM enhancer 3; TFEB,
28 transcriptional factor EB; TFEC, transcription factor EC; V-ATPase, vacuolar-type proton
29 ATPase

30

31 **Abstract**

32 Lysosome is the principal organelle for the ultimate degradation of cellular
33 macromolecules, which are delivered through endocytosis, phagocytosis and autophagy.
34 The lysosomal functions have been found to be impaired by fatty foods and aging, and
35 more importantly, the lysosomal dysfunction in macrophages has been reported as a risk
36 of atherosclerosis development. In this study, we searched for dietary polyphenols which
37 possess the activity for enhancing the lysosomal degradation in J774.1, a murine
38 macrophage-like cell line. Screening test utilizing DQ-BSA digestion identified
39 isorhamnetin (3'-*O*-methylquercetin) as an active compound. Interestingly, structural
40 comparison to inactive flavonols revealed that the chemical structure of the B-ring moiety
41 in isorhamnetin is the primary determinant of its lysosome-enhancing activity.
42 Unexpectedly isorhamnetin failed to inhibit mTORC1-TFEB signaling, a master
43 regulator of lysosomal biogenesis and function. Our data suggested that the other
44 molecular mechanism might be critical for the regulation of lysosomes in macrophages.

45 (145/150 words)

46 **Key words**

47 isorhamnetin, lysosome, polyphenol, macrophage, TFEB

48 **Introduction**

49 The lysosome is an acidic organelle which plays the pivotal role in the
50 degradation of extracellular or intracellular macromolecules. More than 60 kinds of acid
51 hydrolases are identified to function inside lysosomes, which enables to digest a broad
52 range of substrates into catabolites such as amino acids, fatty acids and monosaccharides.
53 Also, it is well known that various kinds of characteristic proteins, including structural
54 proteins like lysosomal-associated membrane protein 1 (LAMP1) family, vacuolar-type
55 proton ATPase (V-ATPase) complexes for the lysosomal acidification, the lysosomal
56 proteases (cathepsins), and soluble N-ethylmaleimide-sensitive-factor attachment protein
57 receptor (SNAREs) that mediate its fusion with other organelles, are essential for the
58 lysosomal functions. ^(1,2)

59 Many reports have demonstrated that the lysosomal dysfunction is associated
60 with the onsets of several diseases. Loss-of-function mutations in lysosomal hydrolases
61 or lysosomal membrane proteins such as β -galactosidase and mucopolipin-1 have been
62 shown to lead to the intracellular accumulation of aberrant lysosomes, which causes
63 Fabry disease and mucopolipidosis type IV, respectively ^(3, 4, 5). Importantly, beside these
64 genetic mutation or deletion, recent reports suggested the possibility that aging and
65 chronic high-fat diet might also attenuate lysosomal proteolysis activity ^(6, 7, 8).

66 Macrophages are professional phagocytic cells which engulf and digest
67 apoptotic cells and exogenous bacteria for the immune response. It is obvious that
68 adequate lysosomal activity is indispensable for macrophages to accomplish the
69 phagocytosis process. Indeed, it has been reported that the genetic deletion of
70 glucocerebrosidase, a lysosomal glycoside hydrolase, impaired endocytosis in
71 macrophages and increased susceptibility to tuberculosis ⁽⁹⁾. Furthermore, Sergin *et al.*

72 found that augmentation of lysosomal activity in macrophages by overexpressing
73 transcriptional factor EB (TFEB), a master regulator of lysosomal biogenesis and function,
74 suppressed the development of aortic root atherosclerosis in apolipoprotein E (ApoE) -
75 knockout mice ⁽¹⁰⁾. These observations suggested that the maintenance of lysosomal
76 function in macrophages might be a potential therapeutic target for these diseases.

77 Polyphenols are plant-derived ingredients with multiple phenol structural units,
78 and we intake them from vegetables and fruits in our daily diet. They are classified into
79 flavonoids, lignans, stilbenes and curcuminoids according to the differences in chemical
80 structures. In particular, flavonoids have been well-studied about their functionality and
81 further classified into nine chemical groups (flavones, flavonols, isoflavones, flavans,
82 flavanols, flavanones, flavanonols, chalcones, and anthocyanidins) ⁽¹¹⁾. Although it is
83 noted that several flavonoids, such as quercetin, kaempferol and epigallocatechin-3-
84 gallate (EGCG), have been reported to enhance autophagy ^(12, 13, 14) in some *in vitro* models,
85 few studies have focused on the lysosomal proteolysis activity in macrophages.

86 Recent studies have identified TFEB as one of the most critical regulators of
87 lysosomal numbers and activities. Under the nutrients-rich condition, TFEB is negatively
88 regulated by mechanistic target of rapamycin complex 1 (mTORC1) in the cytoplasm ⁽¹⁵⁾,
89 whereas amino acids depletion immediately induce TFEB transactivation through
90 mTORC1 inactivation, followed by the upregulation of global gene expressions involved
91 in lysosomal biogenesis and function ⁽¹⁶⁾. Consistent with these studies, Moskot *et al.*
92 showed that the treatment of genistein (4', 5, 7-trihydroxyisoflavone) upregulated some
93 lysosomal gene expressions such as cathepsin F (*Ctsf*) and mucolipin 1 (*Mcoln1*), through
94 TFEB transactivation in Hela cells ⁽¹⁷⁾.

95 In this study, we screened for polyphenol compounds which enhance lysosomal

96 proteolysis in a macrophage-like cell line, J774.1. We then found that the treatment of
97 isorhamnetin (3'-*O*-methylquercetin) significantly activated the lysosomal proteolysis.
98 Additionally, it was also interesting that the chemical structure of B-ring in isorhamnetin
99 were significant for its bioactivity. The potential molecular mechanism of isorhamnetin
100 activity was investigated, which was suggested to be independent on mTORC1-TFEB
101 signaling.

102

103 **Materials and Methods**

104 ***Reagents***

105 Dulbecco's modified eagle medium (DMEM, 4.5 g/L glucose, liquid; 08458-16),
106 penicillin-streptomycin mixed solution (Stabilized; 09367-34), protease inhibitor cocktail,
107 phosphatase inhibitor cocktail (04080-11), and bovine serum albumin (BSA; 01281-26)
108 were obtained from Nacalai Tesque Inc. (Kyoto, Japan). Pronase protease (*Streptomyces*
109 *griseus*; 9036-06-0) was from Sigma-Aldrich (St. Louis, MO, USA). HRP-conjugated
110 antibodies to mouse or rabbit IgG (AP124P or AP124P) were purchased from Millipore
111 Inc. (Billerica, MA, USA). Rabbit polyclonal antibody to Phospho-4E-BP1 (Thr37/46)
112 (236B4; #7547) was from Cell Signaling Technology Inc. (Beverly, MA, USA). Mouse
113 polyclonal antibody to β -Actin (C4; sc-4778) was purchased from Santa Cruz
114 Biotechnology Inc. (Dallas, TX, USA). DQTM Green BSA (D12050) was obtained from
115 Invitrogen (Carlsbad, CA, USA). Fetal bovine serum (FBS; 10270-106) and
116 FluoroBriteTM DMEM (A1896701) was from Thermo Scientific Inc. (Waltham, MA,
117 USA). XfectTM Transfection Reagent (631317) was purchased from Takara Inc. (Kyoto,
118 Japan). Hoechst 33342 (CDX-B0030) was obtained from Chemodex Inc. (St. Gallen,
119 Switzerland). Methanol (25183-70) and acetonitrile (01031-70) were from Kanto

120 Chemical Co. Inc. (Tokyo, Japan). Actinomycin D (014-21261) was purchased from
121 FUJIFILM Wako Pure Chemical Co. (Tokyo, Japan). Bafilomycin A1 (14005) and Torin1
122 (10997) were obtained from Cayman Chemical Co. (Ann Arbor, MI, USA). Polyphenol
123 compounds are obtained by the way shown below. 3'-O-Me-luteolin (1104S), 6-O-Me-
124 luteolin (520-11-6), 7,4'-dihydroxyflavone (1259), datiscetin (1141S), eriodictyol (0056),
125 flavonol (1026), homoeriodictyol (1118S), isoramnetin-3G (1228), isorhamnetin (1120S),
126 kaempferol-3G (1243G), luteolin-7G (1126S), Q3G (0074), quercetagenin (1030),
127 rhamnetin (1136S), tamarixetin (1140S) and tricetin (1335S) were from Extrasynthese
128 (Genay, France). 2,2',4'-trihydroxychalcone (T502), 4,2',5'-trihydroxychalcone (22-314)
129 and gossypetin (G500) were from INDOFINE Chemical Company Inc. (NJ, USA).
130 Flavone (16012-31), morin (23416-31) and pyrogallol (29703-52) were from Nacalai
131 Tesque Inc. (Kyoto, Japan). EGCG (E4268), hyperoside (00180585-25MG) and
132 phloroglucinol (79330-25G) were from Sigma-Aldrich (MO, USA). 1,2,4-
133 trihydroxybenzene, daidzin, piceid, rutin and tangeretin were from Tokyo Chemical
134 Industry Co., Ltd. (Tokyo, Japan). 3,4-dihydroxybenzoic acid, 3,5-dihydroxybenzoic acid,
135 cyanidin, hesperetin and sudachitin were from FUJIFILM Wako Pure Chemical
136 Corporation (Osaka, Japan). Other polyphenols were from natural compound libraries
137 (S990043-NAT1/NAT2) purchased from Sigma-Aldrich (MO, USA).

138

139 ***Cell culture***

140 J774.1, mouse macrophage-like cell line, was obtained from American Type
141 Culture Collection. RAW264.7, mouse macrophage-like cell line, was kindly provided by
142 Dr. T. Nikawa (Tokushima University). They were cultured in DMEM with 10% FBS,
143 penicillin (100 U/mL), and streptomycin (100 µg/mL) at 37°C under humidified 5% CO₂

144 atmosphere.

145

146 ***DQ-BSA degradation assay***

147 DQTM Green BSA (DQ-BSA) was dissolved in phosphate-buffered saline (PBS)
148 to make 1 mg/mL solution. Polyphenol compounds were dissolved in dimethyl sulfoxide
149 (DMSO) to make 10 mM solution. For measurement of degradation products of DQ-BSA
150 in cells, cells were seeded on black-wall clear-bottom 96-well plates (655090; Greiner
151 Bio-One, Frickenhausen, Germany) (6.0×10^4 cells/well) and pre-cultured overnight. They
152 were treated each polyphenol for indicated time with a final DMSO concentration of 0.1%,
153 then added the DQ-BSA solution to a final concentration of 10 μ g/mL. After incubation
154 for 1 h, to quantify fluorescence intensity from digested DQ-BSA, cells were imaged by
155 using Operetta high-content imaging system (PerkinElmer, MA, USA) at 40x
156 magnification at following settings: (λ ex: 460-490 nm, λ em: 500-550 nm). Cell shapes
157 were individually recognized by digital phase contrast and fluorescent intensity in each
158 cell was quantified using dedicated imaging software (Harmony 4.5; PerkinElmer, MA,
159 USA). In the case of using a fluorescent scanner, cells were seeded on 48-well plates
160 (1.2×10^5 cells/well). After treatment with polyphenols and subsequent DQ-BSA, cells
161 were scanned by Typhoon FLA9500 (GE Healthcare, Buckinghamshire, UK) at following
162 settings: (λ ex: 473 nm, λ em: 520-540 nm). To correct differences in cell number during
163 each treatment, cellular proteins were quantified using Protein Assay Bicinchoninic acid
164 Kit (06385-00; Nacalai Tesque, Kyoto, Japan) to yield the ratio of fluorescence intensity/
165 cellular protein amounts.

166 For quantification of degradation products of DQ-BSA in conditioned medium,
167 cells seeded on 12-well plates (6.0×10^6 cells/well) were treated with isorhamnetin (10

168 μM) or Torin1 (1 μM) for 24 h, then incubated with DQ-BSA (final 10 $\mu\text{g}/\text{mL}$) for 4 h.
169 50 μL of conditioned media was added into 450 μL of ice-cold methanol, then incubated
170 at -20°C for 30 min for protein precipitation. After centrifugation (20,600 g, 4°C , 15 min),
171 10 μL of the supernatant was injected into a high-performance liquid chromatography
172 (HPLC) column (0017201; TSKgel ODS-80Ts, 4.6 mm \times 150 mm, Tosoh Bioscience,
173 Tokyo, Japan). The solvent system consisted of 0.1% trifluoroacetic acid (TFA) in 30%
174 acetonitrile and 70% H_2O , and flow rate was 0.8 mL/min. Fluorescence detection was
175 performed at following settings (λ ex: 505 nm, λ em: 515 nm). To prepare *in vitro*
176 degradation products of DQ-BSA, 10 μg of DQ-BSA was incubated with 30 μg of pronase
177 in 100 μL of 50 mM Tris-HCl buffer at 37°C for overnight. The sample was added into
178 800 μL of ice-cold methanol, and incubated at -20°C for 30 min. After centrifugation
179 (20,600 g, 4°C , 15 min), 10 μL of the supernatant was injected into an HPLC column and
180 analyzed in the way described above.

181

182 ***Fluorostaining of intracellular acidic compartment using LysoTracker***

183 Cells were seeded into black-wall clear-bottom 96-well plates. After treatment
184 with isorhamnetin (10 μM) or Torin1, mTOR inhibitor, (1 μM) for 24 h, cells were
185 incubated with LysoTracker® Green DND-26 (L7526; Thermo Scientific, MA, USA)
186 (final 0.5 μM) for 30 min. Following washing with FluoroBrite™ DMEM three times,
187 green fluorescence from LysoTracker inside cells was imaged by using Operetta high-
188 content imaging system at 40x magnification at following settings: (λ ex: 460-490 nm, λ
189 em: 500-550 nm). Fluorescence intensity of each cell was quantified in the way described
190 on DQ-BSA degradation assay.

191

192 ***Fluoroimaging of lysosomal cathepsin B activity***

193 Magic Red® (937; Cosmo Bio, Tokyo, Japan) was dissolved into DMSO/water
194 (1/1). Then, cells were seeded into black-wall clear-bottom 96-well plates. After treatment
195 with isorhamnetin (10 µM) or Torin1 (1 µM) for 24 h, cells were incubated with Magic
196 Red solution (2 µL/well) for 10 min. Following washing with FluoroBrite™ DMEM
197 twice, cells were imaged by using Operetta high-content imaging system at 40x
198 magnification at following settings: (λ ex: 530-560 nm, λ em: 570-650 nm). Red
199 fluorescence intensity from digested Magic Red reagent inside each cell was quantified
200 in the way described above.

201

202 ***Quantitative analyses of flavonols in cells***

203 Cells were seeded on 12-well plates, and treated with each flavonol (10 µM) for
204 1 or 24 h. After washing cells with PBS five times, they were lysed with 300 µL of 1%
205 acetic acid in methanol, containing flavone (10 nM) as an internal standard. Lysates were
206 sonicated for 1 min and centrifuged at 20,600 g for 10 min for protein precipitation, and
207 the supernatants were collected for liquid chromatography tandem mass spectrometry
208 (LC-MS/MS) analyses. Quantitative analyses were performed using HPLC system
209 interfaced to API3200 instrument (SCIEX, MA, USA) working with triple quadrupole
210 analyser in multiple reaction monitoring (MRM) mode. 5 µL of each sample solution was
211 injected into an HPLC column (CD024F; CD-C18 MF, 2 mm×100 mm, Imtakt, Kyoto,
212 Japan). The solvent system consisted of 0.1% FA in H₂O (solvent A) and 0.1% FA in
213 acetonitrile (solvent B). The gradient program was as follows: 0-2 min, 25% B; 2-10 min,
214 linear gradient to 100% B; 10-15 min, 100% B hold; flow rate, 0.2 mL/min. The ESI-MS
215 and MS/MS analysis were performed in negative mode. The ESI-MS source parameters

216 were optimized as follows: curtain gas, 10 psi; ion source gas 1, 30 psi; ion source gas 2,
217 80 psi; temperature, 700°C; and ion spray voltage, -4500 V, collision activated
218 dissociation, 5 psi. The MS/MS transitions of m/z 314.932 \rightarrow 300.000, 314.932 \rightarrow
219 300.000, 284.845 \rightarrow 92.900, 300.849 \rightarrow 151.100, and 316.780 \rightarrow 151.100 were for
220 isorhamnetin, tamarixetin, kaempferol, quercetin and myricetin respectively.

221

222 ***Microscopic observation of intracellular GFP-tagged TFEB***

223 Cells seeded on 12-well plates were transfected with pEGFP-N1-TFEB plasmid
224 (38119; Addgene Inc., MA, USA) using Xfect™ Transfection Reagent. After recovery
225 for 24 h, cells were reseeded into black-wall clear-bottom 96-well plates, and treated with
226 isorhamnetin (10 μ M) or Torin1 (1 μ M) for 1 h. Hoechst 33342 was added into media
227 (final 1 μ g/mL) for staining nuclei, then cells were washed with FluoroBrite™ DMEM
228 twice. Fluorescent image was captured by using Operetta high-content imaging system at
229 40x magnification at following settings: (GFP; λ ex: 460-490 nm, λ em: 500-550 nm,
230 Hoechst 33342; λ ex: 355-385 nm, λ em: 430-500 nm).

231

232 ***Real-time reverse-transcription polymerase chain reaction***

233 Total RNA, prepared using Sepasol®-RNA I Super G (09379-55; Nacalai Tesque,
234 Kyoto, Japan), was reverse transcribed by ReverTra Ace® qPCR RT Master Mix with
235 gDNA Remover (FSQ-301; Toyobo, Osaka, Japan). Then, cDNA was used as template
236 for real-time quantitative polymerase chain reaction (RT-qPCR) analysis with
237 THUNDERBIRD® SYBR qPCR Mix (QPS-201; Toyobo, Osaka, Japan) using
238 LightCycler® Nano System (Roche Diagnostics K.K., Tokyo, Japan). The relative
239 expression of each mRNA was calculated according to the $2^{-\Delta\Delta C_t}$ method. GAPDH was

240 considered as internal control gene. The used primer sequences were as follows: ATPase
241 H⁺ transporting V0 subunit d2 (Atp6v0d2), forward 5'- AAGCCTTTGTTTGACGCTGT
242 -3' and reverse 5'- GCCAGCACATTCATCTGTACC -3'; cathepsin D (Ctsd), forward 5'-
243 CTGAGTGGCTTCATGGGAAT -3' and reverse 5'- CCTGACAGTGGAGAAGGAGC -
244 3'; glyceraldehyde-3-phosphate dehydrogenase (Gapdh), forward 5'-
245 GTGAAGGTCGGAGTCAACG -3' and reverse 5'- TGAGGTCAATGAAGGGGTC -3';
246 lysosomal-associated membrane protein 2a (Lamp2a), forward 5'-
247 GCAGTGCAGATGAAGACAAC -3' and reverse 5'- AGTATGATGGCGCTTGAGAC -
248 3'.

249

250 ***Western blotting***

251 Cells were washed with PBS, and lysed in a radio-immunoprecipitation assay
252 buffer [50 mM Tris-HCl (pH 7.4), 150 mM NaCl, 0.25% deoxycholic acid, 1% NP-40,
253 0.1% sodium dodecyl sulfate (SDS), 1 mM ethylenediaminetetraacetic acid]
254 supplemented with both protease and phosphatase inhibitor cocktails. The protein
255 concentrations in cell lysates were measured by BCA assay. Proteins were separated on a
256 10% SDS/polyacrylamide gel, then transferred to Immobilon-P PVDF membranes
257 (IPVH00010; Millipore, MA, USA). The membrane was blocked with EzBlock Chemi
258 (2332615; Atto Corp., Tokyo, Japan) at room temperature for 30 min, then probed with a
259 primary antibody (1:1000) in Tris-buffered saline with 0.05% Tween 20 (TTBS)
260 containing 5% BSA at 4 °C overnight. After washing with TTBS, they were incubated in
261 solution containing secondary antibody conjugated with horseradish peroxidase (1:2000)
262 at room temperature for 75 min. After washing, chemiluminescent detection was
263 performed using Chemi-Lumi One or Chemi-Lumi One Super (07880, 02230; Nacalai

264 Tesque, Kyoto, Japan) and visualized by Ex-Capture MG (Atto Corp., Tokyo, Japan).

265

266 ***Statistical analysis***

267 All data were expressed as means \pm SEM. Statistical analysis were performed using *t*-test
268 or one-way analysis of variance (ANOVA). When ANOVA indicated a significant
269 difference among groups, these groups were compared by Dunnett's or Tukey's test. All
270 statistical analyses were performed using Prism 5 (GraphPad Software, CA). The
271 threshold for statistical significance was set at $p < 0.05$.

272

273 **Results**

274 ***Screening of dietary polyphenols which enhance lysosomal proteolysis in J774.1 cells***

275 First, we attempted to establish a cell-based system to measure the activity of
276 lysosomal proteolysis. We used DQ-BSA, BSA protein chemically modified with a kind
277 of boron dipyrromethene (BODIPY) dye, for the assay system. This reagent is designed
278 to be internalized into the cytoplasm to be degraded in lysosomes eventually, which is
279 accompanied by the robust increase of fluorescence emission. DQ-BSA treatment to
280 J774.1 mouse macrophage-like cells immediately increased the intracellular green
281 fluorescence [Fig. 1a], suggesting its proteolytic degradation. To confirm whether the
282 fluorescence intensity is indeed available as a quantitative indicator of lysosomal activity,
283 we quantified the cellular fluorescence intensity after pre-treatment with Torin1, an
284 mTOR inhibitor, which had been reported to facilitate DQ-BSA degradation in several
285 cultured cell lines, and bafilomycin A1 (BAF), a chemical inhibitor of lysosomal
286 acidification^(18, 19) [Fig. 1a and b]. Expectedly, inhibition of lysosomal activity by BAF
287 treatment resulted in the remarkable reduction of DQ-BSA-derived fluorescence, whereas

288 Torin1 significantly increased the intensity similarly to the previous reports.

289 Then, 56 kinds of dietary polyphenols, including flavonol, catechin, flavanone,
290 anthocyanidin, flavanol, flavone, stilbene, isoflavone and chalcone, were treated to J774.1
291 cells respectively for the assessment of their effects on the lysosomal proteolysis (n=1).
292 This screening test was performed at 10 μ M concentration for all compounds because few
293 of them showed cytotoxicity at up to this concentration upon 24 h treatment [data not
294 shown]. We found that the treatment of a few flavonol compounds, including
295 isorhamnetin, tended to enhance DQ-BSA degradation [Fig. 1c]. To verify the inducing
296 activity of isorhamnetin on this assay system, we further performed DQ-BSA assay under
297 several different experimental conditions, which revealed that treatment of isorhamnetin
298 at relatively high concentrations (10 or 20 μ M) significantly enhanced DQ-BSA
299 degradation [Fig. 1d]. Additionally, it was found that its treatment for a shorter time (1-
300 12 h) was not fully effective to enhance DQ-BSA digestion [Fig. 1e]. These results
301 demonstrated that 24 h treatment of isorhamnetin, a kind of dietary flavonols, promote
302 lysosomal proteolysis in J774.1.

303

304 ***Isorhamnetin activated lysosomal functions in J774.1 cells.***

305 Given the possibility that isorhamnetin may enhance DQ-BSA intake through
306 endocytosis as well as its lysosomal proteolysis, we attempted to assess the lysosomal
307 properties by using other methodologies. Staining cells with lysotracker revealed that the
308 area of acidic compartments per cell were significantly increased by isorhamnetin
309 treatment [Fig. 2a and b], suggesting increased number of lysosomes. Regarding the
310 proteolytic activity of lysosomes, the enzymatic activity of cathepsin B, one of lysosomal
311 cysteine proteases, was evaluated by using a fluorescent substrate, Magic Red, showing

312 its significant activation by isorhamnetin treatment [Fig. 2c and d].

313 Interestingly, we also found that conditioned media of J774.1 cells treated with
314 DQ-BSA emitted the remarkable green fluorescence, implying that the degradation
315 products of DQ-BSA might be partly secreted into the media. To validate this hypothesis,
316 we established another analytical methodology using HPLC-Fluorescence system which
317 is capable to detect the final proteolytic products of DQ-BSA specifically. Proteolytic
318 product of DQ-BSA, yielded by the *in vitro* incubation with pronase, was successfully
319 detected as a single peak by the HPLC-Fluorescence analysis [Fig. 2e]. Expectedly,
320 conditioned media of cells treated with DQ-BSA was found to contained fluorescent
321 molecules with an almost identical retention time [Fig. 2f], and it was also notable that
322 isorhamnetin treatment increased its extracellular secretion [Fig. 2g]. Furthermore, we
323 confirmed that the enhancement of DQ-BSA degradation by isorhamnetin was observed
324 in other mouse macrophage-like cell line, RAW264.7 [Fig. 2h]. These results confirmed
325 that isorhamnetin treatment on murine macrophage-like cells led to the lysosomal
326 activation.

327

328 ***3'-Methoxy group in B-ring moiety is critical for isorhamnetin activity***

329 Based on the screening test shown in Figure 1c, isorhamnetin, a flavonol
330 compound possessing mono-methoxylated B-ring, seemed to be the most effective among
331 56 candidates. Focusing on its characteristic structure of B-ring, the activities of 4 other
332 flavonols with slightly differed B-ring (tamarixetin, kaempferol, quercetin and myricetin;
333 Fig. 3a) were re-evaluated in triplicate by DQ-BSA assay. Intriguingly, these flavonol
334 compounds, whose B-ring moieties were structurally varied, were shown to be inactive
335 regarding to lysosomal proteolysis [Fig. 3b]. This result indicated the biological

336 significance of the chemical structure, 3'-methoxy-4'-hydroxy groups, on B-ring moiety
337 in isorhamnetin.

338 Since the molecular polarities and stabilities of these 5 flavonols were speculated
339 to be slightly differed, we attempted to quantify the amount of each compound
340 accumulated in the cells after 1 or 24 h treatment. LC-MS/MS analysis of cell lysates
341 revealed that 4 kinds of flavonols other than myricetin were interacted with cells after 1
342 h treatment. After 24 h treatment, quercetin was markedly reduced, whereas compounds
343 with relatively hydrophobic B ring moiety, isorhamnetin, tamarixetin, and kaempferol,
344 kept interacted with cells. [Fig. 3c and d]. It was noted that tamarixetin and kaempferol
345 seemed to possess higher affinities for cells in spite of their less activities. It was also
346 interesting that small amounts of isorhamnetin (0.07 ± 0.006 nmol/mg protein; 1 h,
347 0.01 ± 0.003 nmol/mg protein; 24 h) were detected in cells treated with quercetin,
348 suggesting the *O*-methylation by catechol *O*-methyl transferase⁽²⁰⁾. On the other hand,
349 glucuronide or sulfate conjugates of these flavonols were not detected by HPLC-UV
350 analyses (data not shown), indicating that these polyphenolic compounds are scarcely
351 metabolized by conjugation reactions in this macrophage-like cell line, which has been
352 reported to express β -glucuronidase to deconjugate flavonoid glucuronides⁽²¹⁾.

353 These data suggest that a certain degree of hydrophobicity of B ring moiety is
354 required to interact with cells, and 3'-methoxylated structure is critical for inducing
355 lysosomal activation.

356

357 ***Isorhamnetin did not induce TFEB transactivation.***

358 We next attempted to investigate the molecular mechanism underlying the
359 inducing effects of isorhamnetin on lysosomal activity. The time-course experiment

360 shown in Figure 1e had revealed that 24 h treatment with isorhamnetin was indispensable
361 for exhibiting its activity, which strongly suggested the modulation of gene expressions
362 might be involved in the mechanisms. Consistent with this hypothesis, co-treatment of
363 actinomycin D, an inhibitor of RNA synthesis, completely canceled the lysosomal
364 activation induced by isorhamnetin treatment [Fig. 4a]. Taken together, altering gene
365 expressions is considered to be essential for the lysosomal activation by isorhamnetin.

366 Considering the upstream mechanism of mRNA upregulation by isorhamnetin,
367 we focused on TFEB, a transcriptional factor known as a master regulator of lysosomal
368 biogenesis, whose activation has been reported to be controlled by mTORC1 signaling.
369 To examine TFEB transactivation, we first observed its cellular localization in J774.1
370 cells. Fluoroimaging cells expressing TFEB tagged by GFP revealed its diffused
371 localization in cytoplasm. Unexpectedly, isorhamnetin treatment scarcely promote the
372 nuclear translocation of GFP-TFEB while its nuclear translocation was obviously seen in
373 Torin1-treated cells [Fig. 4b]. On the other hand, lysosomal gene expressions such as
374 *Atp6vod2*, *Ctsd* and *Lamp2a* were confirmed to be upregulated by overexpression of a
375 constitutively active mutant form of TFEB (TFEB-S3A/R4A) [Fig. 4c]. Importantly,
376 mRNA expressions of these TFEB target genes were not induced by isorhamnetin
377 treatment whereas Torin1 treatment significantly increased their expressions [Fig. 4d].
378 Furthermore, isorhamnetin scarcely altered phosphorylation level of 4E-BP1, an
379 mTORC1 substrate, in contrast to Torin1 [Fig. 4e]. These data showed mTORC1-TFEB
380 signaling is not modulated by isorhamnetin, and suggested the possibility that lysosomal
381 functions in J774.1 macrophages could be regulated partly through the distinct
382 mechanism from TFEB-related pathway.

383

384 **Discussion**

385 Lysosome plays the pivotal role in the ultimate degradation on the catabolic
386 processes through the endocytic and autophagic pathways. Whereas the effects of several
387 dietary polyphenols on autophagy have been recently studied ^(12, 13, 14), there has been few
388 reports paying attention to their effects on the lysosomal function. In this study, we
389 performed the screening test on 56 kinds of compounds to find out dietary polyphenols
390 which enhance the lysosomal proteolysis and identified isorhamnetin as an active
391 compound.

392 Regarding the bioactivities of natural polyphenolic compounds, anti-oxidant and
393 anti-inflammatory effects have been widely studied by both *in vitro* & *in vivo* experiments.
394 Most of previous reports have shown that the anti-oxidant and anti-inflammatory activity
395 of isorhamnetin was lower than that of quercetin, a 3'-*O*-demethylated derivative, due to
396 lack of catechol structure ^(22, 23). Interestingly, our present study described that the effect
397 of enhancing lysosomal activity was seen in only isorhamnetin rather than quercetin. This
398 result strongly suggests that the molecular mechanism underlying the lysosomal
399 activation by isorhamnetin is independent on its anti-oxidant and anti-inflammatory
400 activities. Moreover, our study also indicated that the chemical structure of 3'-methoxy-
401 4'-hydroxy groups on B-ring moiety is critical for isorhamnetin activity. Considering
402 these results, the lysosomal activation by isorhamnetin may require its physiological
403 interaction to a specific intracellular molecule; that is to say, a certain key molecule may
404 be interacted with isorhamnetin specifically and acting as its functional target in this
405 cultured cell model.

406 Isorhamnetin is a bioactive compound derived from herbal medicinal plants or
407 vegetables such as potherb mustards, radish leaves and apples (without peels) ⁽²⁴⁾. It has

408 been reported to possess multiple bioactivities like suppressive effects on arteriosclerosis
409 in Apo-E knockout mice fed a high fat diet and adipocyte differentiation induced by
410 rosiglitazone, a peroxisome proliferator-activated receptor γ (PPAR γ) agonist, in 3T3-L1
411 cells^(25,26). Considering its low availability from dietary intake, it seems to be difficult to
412 orally take sufficient amount of isorhamnetin, since its content in vegetables was shown
413 to be much lower than quercetin, which is widely contained in vegetables. For instance,
414 the total content of isorhamnetin glycosides in onion were reported to be approximately
415 8-22 mg/100 g DW whereas that of quercetin glycosides were 171-294 mg/100 g DW⁽²⁷⁾.
416 However, it is worth noting that isorhamnetin has also been identified as a metabolite of
417 quercetin in mammalian serum, which is transformed through the methylation reaction at
418 3'-hydroxy group on B-ring by catechol-*O*-methyl-transferase mainly in the liver tissue.
419 Indeed, serum concentration of isorhamnetin in mice has been reported to reach to
420 approximately 2 μ M after 6 weeks of feeding a diet supplemented with quercetin (2 mg/g)
421⁽²⁸⁾. These reports suggest the possibility of quercetin as a potent and practical activator
422 of lysosome in *in vivo* models.

423 This study investigated the molecular mechanisms underlying the lysosomal
424 activation in isorhamnetin-treated J774.1 cells. Although data demonstrated that *de novo*
425 gene expressions are closely involved in the mechanism, isorhamnetin treatment failed to
426 promote TFEB nuclear translocation and the subsequent upregulation of lysosomal gene
427 expressions such as *Atp6v0d2*, *Ctsd* and *Lamp2a*. Consistent with these results,
428 isorhamnetin treatment also failed to repress the kinase activity of mTORC1, a negative
429 regulator of TFEB transactivation. These data suggested that TFEB is not responsible for
430 the mechanism of lysosomal activation by isorhamnetin in this cell line. Importantly,
431 TFEB belongs to the MITF/TFE family of transcription factors that includes

432 microphthalmia-associated transcription factor (MITF), transcription factor binding to
433 IGHM enhancer 3 (TFE3) and transcription factor EC (TFEC), and these 4 transcription
434 factors have been reported to share the role in regulating similar series of lysosomal genes
435 (29, 30, 31). However, it is predictable that 3 transcription factors other than TFEB are not
436 participating in the mechanism of isorhamnetin, since the transactivation of these
437 MITF/TFE families are found to be commonly controlled by mTORC1 signaling,
438 similarly to that of TFEB.

439 A previous report has described that treatment with genistein, one of the dietary
440 isoflavone, upregulated lysosomal related gene expressions such as cathepsin F and
441 mucolipin 1, and promoted lysosomal biogenesis through TFEB transactivation in HeLa
442 cells⁽¹⁷⁾. Although genistein has also been tested in our screening assay [Fig. 1c], it didn't
443 facilitate the lysosomal degradation of DQ-BSA in J774.1 cells. The higher concentration
444 (50 μ M) of genistein, compared with the previous report, also failed to activate lysosomal
445 function in our assay [data not shown]. These observations strongly supported our
446 prediction that unknown mechanisms independent on TFEB or MITF/TFE family are critical
447 for the lysosomal regulation in J774.1 macrophages.

448 In summary, our results indicate that isorhamnetin activates lysosomal function
449 in J774.1, and the molecular mechanism is not related to mTORC1-TFEB signaling. It is
450 likely that future studies on isorhamnetin will lead to the identification of the novel critical
451 signaling pathway for the lysosomal regulation in macrophages.

452

453 **Author contributions**

454 K. O. and Y. T. designed and supervised this study. M. S. performed the experiments. M.
455 M., H. O., H. Y-O., and T. H. assisted with the experiments and contributed to the

456 discussions. M. S. wrote the manuscript with the assistance of K. O. and Y. T..

457

458 **Disclosure statement**

459 No potential conflict of interest was reported by the authors.

460

461 **Acknowledgement**

462 We sincerely thank Dr. Takeshi Nikawa for kindly providing us with RAW264.7
463 cells, and appreciate Fujii Memorial Institute of Medical Sciences for sharing the use of
464 Operetta high-content imaging system and Typhoon FLA9500. We also thank Ms. Satoko
465 Nakano and Ms. Akiko Uebanso for their support and encouragement for this work. This
466 study was supported by Japan Society for the Promotion of Science [KAKENHI Grant
467 Number 13J09070, 26660110, & 18K14422].

468

469 **References**

- 470 1) Haoxing X, Dejian R. Lysosomal Physiology. *Annu Rev Physiol.* 2015;77:57-80
- 471 2) Appelqvist H, Wäster P, Kågedal K, Öllinger K, et al. The lysosome: from waste bag
472 to potential therapeutic target. *J Mol Cell Biol.* 2013;5:214-226
- 473 3) Haskins ME, Giger U, Patterson DF, et al. Animal models of lysosomal storage
474 diseases: their development and clinical relevance. *Oxford PharmaGenesis.*
475 2006;455:56-62
- 476 4) Hers HG. alpha-Glucosidase deficiency in generalized glycogenstorage disease
477 (Pompe's disease). *Biochemical Journal.* 1963;86:11-16
- 478 5) Sun M, Goldin E, Stahl S, Falardeau JL, Kennedy JC, Acierno JS Jr, Bove C, Kaneski
479 CR, Nagle J, Bromley MC, Colman M, Schiffmann R, Slaugenhaupt SA, et al.

- 480 Mucopolidosis type IV is caused by mutations in a gene encoding a novel transient
481 receptor potential channel. *Hum Mol Genet.* 2000;9:2471-2478
- 482 6) Huang J, Xu J, Pang S, Bai B, Yan B, et al. Age-related decrease of the LAMP-2 gene
483 expression in human leukocytes. *Clinical biochemistry.* 2012;45:1229-1232
- 484 7) Papáčková Z, Daňková H, Páleníčková E, Kazdová L, Cahová M, et al. Effect of
485 short- and long-term high-fat feeding on autophagy flux and lysosomal activity in rat
486 liver. *Physiol. Res.* 2012;61:S67-76
- 487 8) Yamamoto T, Takabatake Y, Takahashi A, Kimura T, Namba T, Matsuda J, Minami S,
488 Kaimori JY, Matsui I, Matsusaka T, Niimura F, Yanagita M, Isaka Y, et al. High-Fat
489 Diet-Induced Lysosomal Dysfunction and Impaired Autophagic Flux Contribute to
490 Lipotoxicity in the Kidney. *J Am Soc Nephrol.* 2017;28:1534-1551
- 491 9) Berg RD, Levitte S, O'Sullivan MP, O'Leary SM, Cambier CJ, Cameron J, Takaki KK,
492 Moens CB, Tobin DM, Keane J, Ramakrishnan L, et al. Lysosomal Disorders Drive
493 Susceptibility to Tuberculosis by Compromising Macrophage Migration. *Cell.*
494 2016;165: 39-152
- 495 10) Sergin I, Evans TD, Zhang X, Bhattacharya S, Stokes CJ, Song E, Ali S, Dehestani B,
496 Holloway KB, Micevych PS, Javaheri A, Crowley JR, Ballabio A, Schilling JD,
497 Epelman S, Wehl CC, Diwan A, Fan D, Zayed MA Razani B, et al. Exploiting
498 macrophage autophagy-lysosomal biogenesis as a therapy for atherosclerosis. *Nat*
499 *Commun.* 2017;8:15750
- 500 11) An-Na L ,Sha L,Yu-Jie Z,Xiang-Rong X, Yu-Ming C, Hua-Bin L, et al. Resources
501 and biological activities of natural polyphenols. *Nutrients.* 2014;6:6020-47
- 502 12) Kim H, Moon JY, Ahn KS, Cho SK, et al. Quercetin induces mitochondrial mediated
503 apoptosis and protective autophagy in human glioblastoma U373MG cells. *Oxid Med*

- 504 Cell Longev. 2013;2013:596496
- 505 13) Huang WW, Tsai SC, Peng SF, Lin MW, Chiang JH, Chiu YJ, Fushiya S, Tseng MT
506 Yang JS, et al. Kaempferol induces autophagy through AMPK and AKT signaling
507 molecules and causes G2/M arrest via downregulation of CDK1/cyclin B in SK-HEP-
508 1 human hepatic cancer cells. *Int J Oncol.* 2013;42:2069-2077
- 509 14) Holczer M, Besze B, Zámbo V, Csala M, Bánhegyi G, Kapuy O, et al.
510 Epigallocatechin-3-Gallate (EGCG) Promotes Autophagy-Dependent Survival via
511 Influencing the Balance of mTOR-AMPK Pathways upon Endoplasmic Reticulum
512 Stress. *Oxid Med Cell Longev.* 2018;2018:6721530
- 513 15) Settembre C, Zoncu R, Medina DL, Vetrini F, Erdin S, Erdin S, Huynh T, Ferron M,
514 Karsenty G, Vellard MC, Facchinetti V, Sabatini DM, Ballabio A, et al. A lysosome-
515 to-nucleus signalling mechanism senses and regulates the lysosome via mTOR and
516 TFEB. *EMBO Journal.* 2012;31:1095-1108
- 517 16) Settembre C, Di Malta C, Polito VA, Garcia Arencibia M, Vetrini F, Erdin S, Erdin
518 SU, Huynh T, Medina D, Colella P, Sardiello M, Rubinsztein DC, Ballabio A, et al.
519 TFEB links autophagy to lysosomal biogenesis. *Science.* 2011;332:1429-1433
- 520 17) Moskot M, Montefusco S, Jakóbkiewicz-Banecka J, Mozolewski P, Węgrzyn A, Di
521 Bernardo D, Węgrzyn G, Medina DL, Ballabio A, Gabig-Cimińska M, et al. The
522 phytoestrogen genistein modulates lysosomal metabolism and transcription factor EB
523 (TFEB) activation. *J. Biol. Chem.* 2014;289:17054-17069
- 524 18) Palm W, Park Y, Wright K, Pavlova NN, Tuveson DA, Thompson CB, et al. The
525 Utilization of Extracellular Proteins as Nutrients Is Suppressed by mTORC1. *Cell.*
526 2015;162:59-270
- 527 19) Zullo, AJ, Jurcic Smith KL, Lee S, et al. Mammalian target of Rapamycin inhibition

528 and mycobacterial survival are uncoupled in murine macrophages. BMC biochemistry.
529 2014;15:4

530 20) Zhu BT, Ezell EL, Liehr JG, et al. Catechol-O-methyltransferase-catalyzed rapid O-
531 methylation of mutagenic flavonoids. Metabolic inactivation as a possible reason for
532 their lack of carcinogenicity in vivo. J Biol Chem. 1994;269(1):292-299

533 21) Terao J. Factors modulating bioavailability of quercetin-related flavonoids and the
534 consequences of their vascular function. Biochem Pharmacol. 2017;139:15-23

535 22) Duen~as D, Surco-Laos F, Gonza´lez-Manzano S, Gonza´lez-Parama´s AM, Santos-
536 Buelga C, et al. Antioxidant properties of major metabolites of quercetin. Eur. Food
537 Res. Technol. 2011;232:103-111

538 23) Hämäläinen M, Nieminen R, Vuorela P, Heinonen M, Moilanen E, et al. Anti-
539 inflammatory effects of flavonoids: genistein, kaempferol, quercetin, and daidzein
540 inhibit STAT-1 and NF-kappaB activations, whereas flavone, isorhamnetin,
541 naringenin, and pelargonidin inhibit only NF-kappaB activation along with their
542 inhibitory effect on iNOS expression and NO production in activated macrophages.
543 Mediators Inflamm. 2007;2007:45673.

544 24) Cao J, Chen W, Zhang Y, Zhang Y, Zhao X, et al. Content of Selected Flavonoids in
545 100 Edible Vegetables and Fruits. Food Sci. Technol. Res. 2010;16:395-402

546 25) Luo Y, Sun G, Dong X, Wang M, Qin M, Yu Y, Sun X, et al. Isorhamnetin attenuates
547 atherosclerosis by inhibiting macrophage apoptosis via PI3K/AKT activation and
548 HO-1 induction. PLoS One. 2015;10:e0120259

549 26) Zhang Y, Gu M, Cai W, Yu L, Feng L, Zhang L, Zang Q, Wang Y, Wang D, Chen H,
550 Tong Q, Ji G, Huang C, et al. Dietary component isorhamnetin is a PPARγ antagonist
551 and ameliorates metabolic disorders induced by diet or leptin deficiency. Scientific

- 552 Reports. 2016;6:19288
- 553 27) Lee J, Mitchell AE. Quercetin and isorhamnetin glycosides in onion (*Allium cepa* L.):
554 varietal comparison, physical distribution, coproduct evaluation, and long-term
555 storage stability. *J Agric Food Chem.* 2011;59:857-863
- 556 28) Boesch-Saadatmandi C, Egert S, Schrader C, Coumoul X, Barouki R, Muller MJ,
557 Wolfram S, Rimbach G, et al. Effect of quercetin on paraoxonase 1 activity--studies
558 in cultured cells, mice and humans. *J Physiol Pharmacol.* 2010;61:99-105
- 559 29) Yang M, Liu E, Tang L, Lei Y, Sun X, Hu J, Dong H, Yang SM, Gao M, Tang B, et al.
560 Emerging roles and regulation of MiT/TFE transcriptional factors. *Cell Commun*
561 *Signal.* 2018;16:31
- 562 30) Martina JA, Diab HI, Lishu L, Jeong-AL, Patange S, Raben N, Puertollano R, et al.
563 The nutrient-responsive transcription factor TFE3 promotes autophagy, lysosomal
564 biogenesis, and clearance of cellular debris. *Sci Signal.* 2014;7:ra9
- 565 31) Ploper D, Taelman VF, Robert L, Perez BS, Titz B, Chen HW, Graeber TG, von Euw
566 E, Ribas A, De Robertis EM, et al. MITF drives endolysosomal biogenesis and
567 potentiates Wnt signaling in melanoma cells. *Proc Natl Acad Sci U S A.*
568 2015;112:E420-9

569

570 **Figure 1 Screening test revealed that isorhamnetin enhanced DQ-BSA degradation.**

571 J774.1 cells were treated with Torin1 (1 μ M) for 24 h, then incubated with DQ-BSA (10 μ g/mL) for 1
572 h with/without bafilomycin A1 (100 nM) (a and b). Cells were treated with 56 kinds of polyphenolic
573 compounds (10 μ M each) for 24 h, then DQ-BSA was added to quantify the lysosomal proteolysis (c).
574 Cells were treated with isorhamnetin at indicated concentrations for 24 h prior to DQ-BSA exposure
575 (d). Cells were treated with isorhamnetin at 10 or 20 μ M for different h as indicated prior to DQ-BSA

576 exposure (e). Green fluorescence inside cell was imaged and quantified using Operetta CLS™ and
577 Harmony 4.5 (a-c) or Typhoon FLA9500 (d and e). Relative fluorescence intensities to DMSO control
578 were graphed (b-e). Data represent means ± SEM of triplicate determinations (b, d and e). Different
579 letters indicate significant differences by Tukey-Kramer test ($p < 0.05$) (b). Statistical significance was
580 analyzed using Dunnett's test ($*p < 0.05$) (d and e). Abbreviations of polyphenolic compounds in figure
581 1c are as follows: 3G; 3-glucoside, Q; quercetin, EGCG; epigallocatechin gallate, ECG; epicatechin
582 gallate, EGC; epigallocatechin, EC; epicatechin, 7G; 7-glucosidice, Me; methyl.

583

584 **Figure 2 Isorhamnetin enhances the lysosomal number and proteolytic function.**

585 J774.1 cells were treated with isorhamnetin (10 μM) or Torin1 (1 μM) for 24 h, then incubated with
586 lysotracker (0.5 μM) for 30 min (a) or Magic Red® (2 μL/well) for 10 min (c). Fluorescence
587 intensities inside cells were imaged and quantified by using Operetta CLS™ and Harmony 4.5 (b and
588 d). Degradation products of DQ-BSA by pronase digestion were detected by HPLC-fluorescence
589 analysis (e). Cells were treated with isorhamnetin (10 μM) or Torin1 (1 μM) for 24 h, then incubated
590 with DQ-BSA (10 μg/mL) for 1 h. Conditioned media were analyzed by HPLC-fluorescence analysis,
591 and digested DQ-BSA was quantified (f and g). RAW264.7 cells were treated with isorhamnetin (10
592 μM) or Torin1 (1 μM) for 24 h, then incubated with DQ-BSA (10 μg/mL) for 1 h. The fluorescence
593 was quantified in the same way as Figure 1 (a) and (b), and relative fluorescence intensities to DMSO
594 control were graphed (h). Data represent means ± SEM of triplicate determinations. Statistical
595 significance was analyzed using the Dunnett's test ($*p < 0.05$) (b, d, g and h).

596

597 **Figure 3 Structure-activity relationship of isorhamnetin for the lysosomal activation.**

598 Chemical structures of isorhamnetin and other 4 flavonols with varied B-ring moieties are shown (a).
599 Cells were treated with indicated flavonols (10 μM each) for 24 h, then incubated with DQ-BSA (10

600 $\mu\text{g/mL}$) for 1 h. Intensities of cellular green fluorescence were quantified by Typhoon FLA9500 (b).
601 Cells were treated with each flavonol (10 μM) for 1 or 24 h, and their amounts accumulated in cells
602 were quantified by LC-MS/MS analysis (c). The relative amounts of flavonols after 24 h treatment to
603 1 h treatment were shown (d). Data represent means \pm SEM of triplicate determinations (b-d).
604 Different letters indicate significant differences by Tukey-Kramer test ($p < 0.05$) (b and d). Statistical
605 significance was assessed using unpaired *t*-test ($*p < 0.05$) (c).

606

607 **Figure 4 mTORC1-TFEB signaling is not activated by isorhamnetin treatment.**

608 Cells were treated with isorhamnetin (10 μM) with/without actinomycin D (5 μM) for 24 h. After DQ-
609 BSA exposure, cellular fluorescence intensities were quantified by Typhoon FLA9500 (a). GFP-TFEB
610 expressing cells were treated with isorhamnetin (10 μM) or Torin1 (1 μM) for 1 h, then nuclei were
611 stained with Hoechst33342. Cellular fluorescence was imaged by using Operetta CLS™ (b). Relative
612 mRNA expressions of indicated lysosomal genes in cells overexpressing constitutively activated
613 TFEB (TFEB-S3A/R4A) (c). Relative mRNA expressions of TFEB target genes after the incubation
614 with isorhamnetin (10 μM) for 8 h (d). Phosphorylated forms of 4E-BP1 in cells treated with
615 isorhamnetin (10 μM) or Torin1 (1 μM) for 1 h (e). Data represent means \pm SEM of triplicate
616 determinations (a, c and d). Different letters indicate significant differences by Tukey-Kramer test
617 ($p < 0.05$) (a). Statistical significance was analyzed using Dunnett's test ($*p < 0.05$)

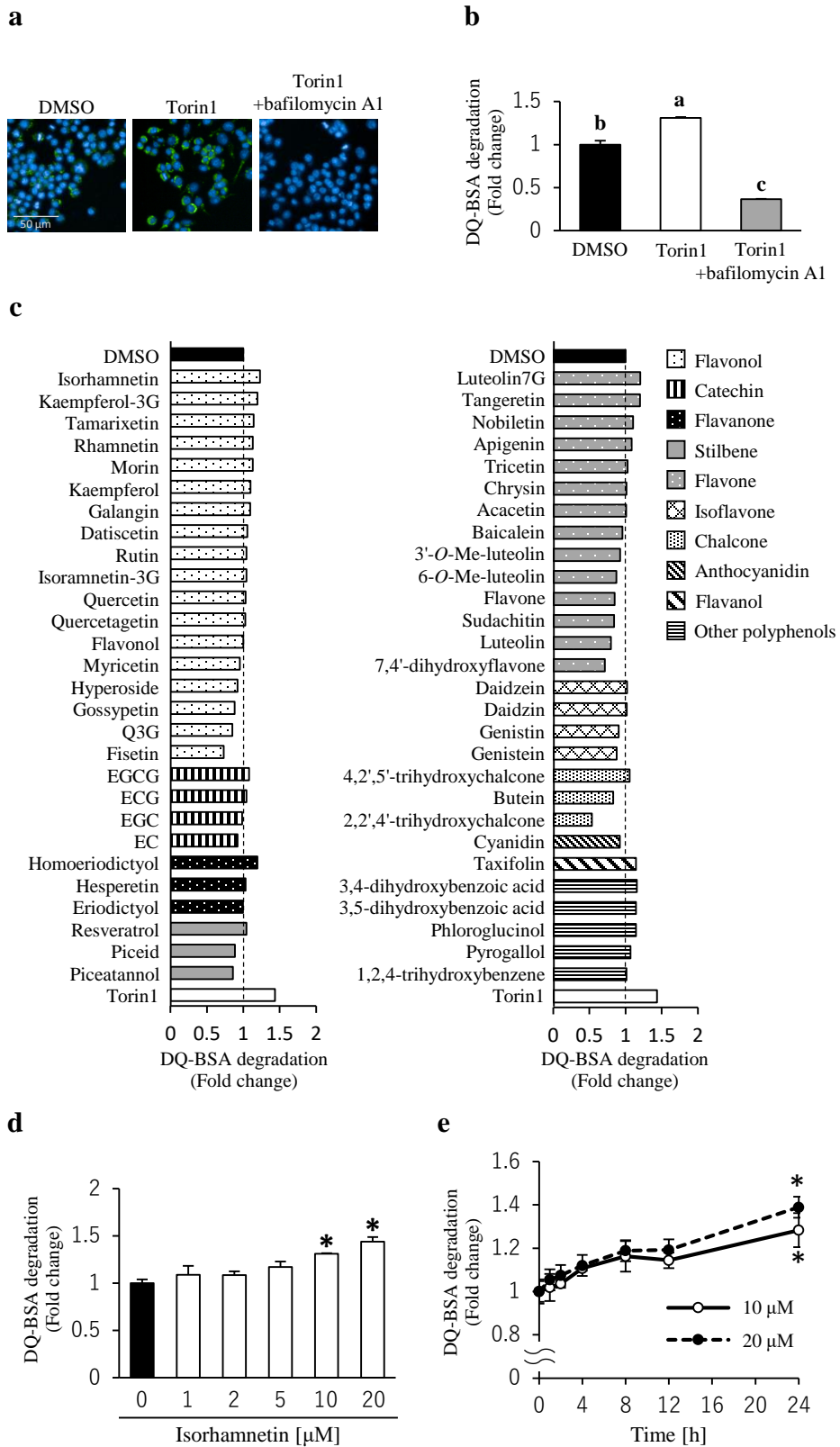


Figure 1, Sakai M *et al.*

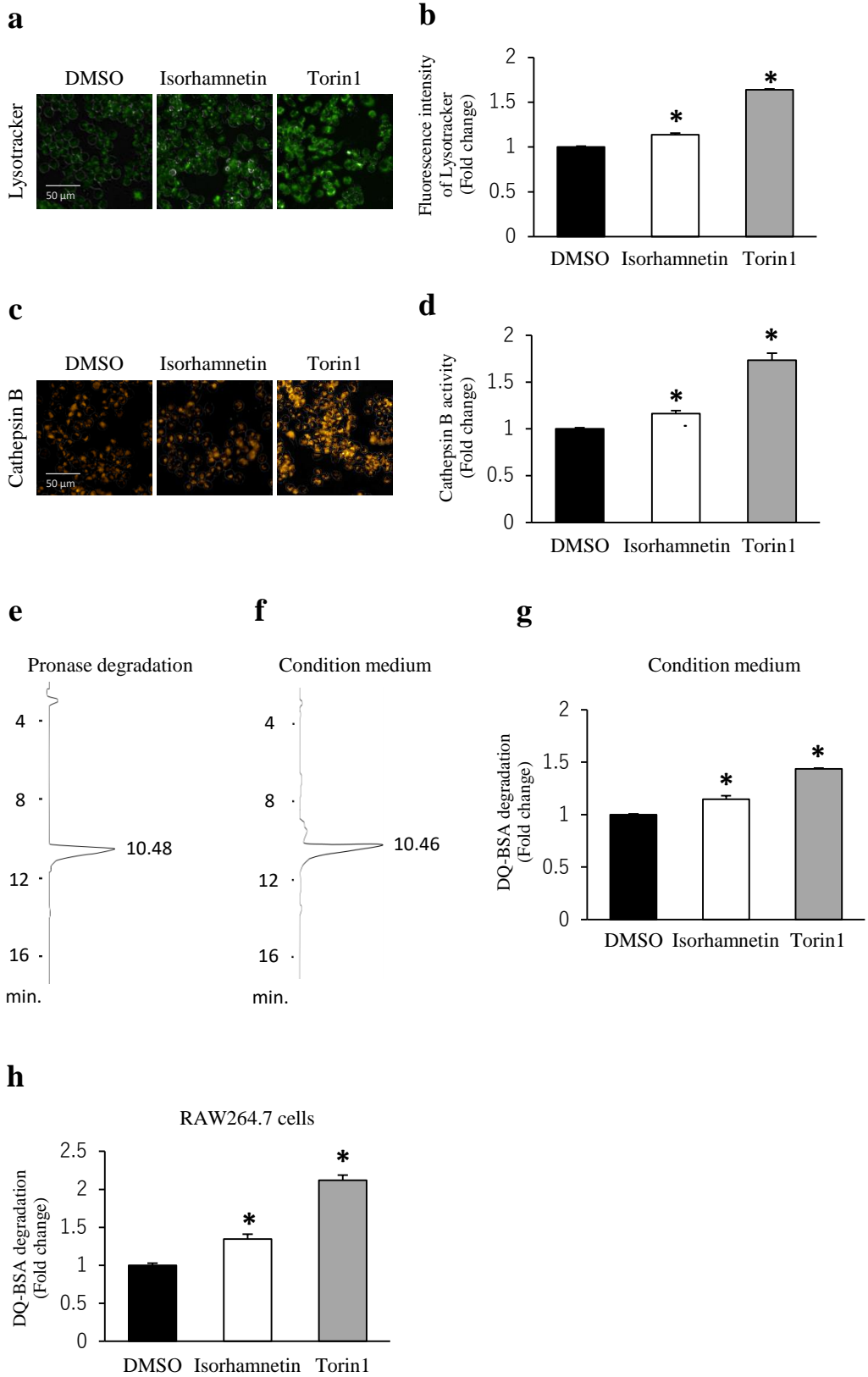
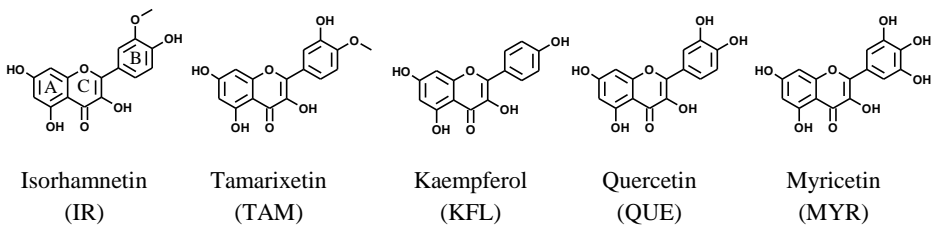
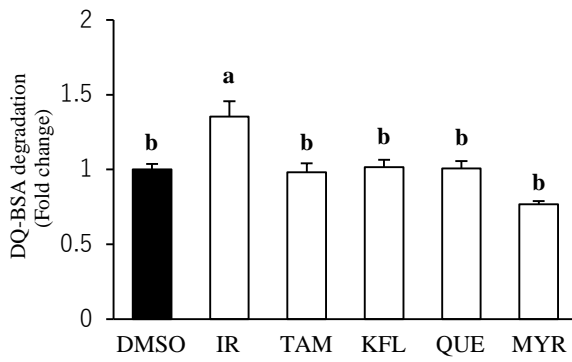


Figure 2, Sakai M *et al.*

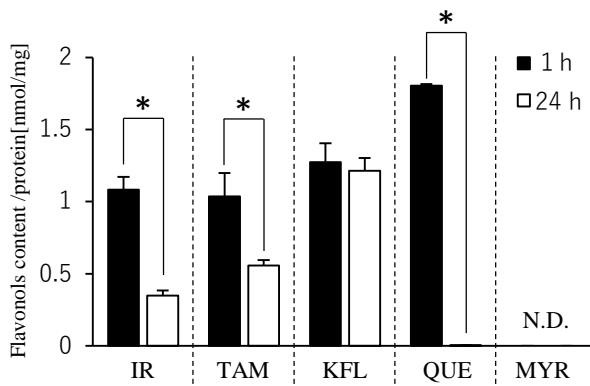
a



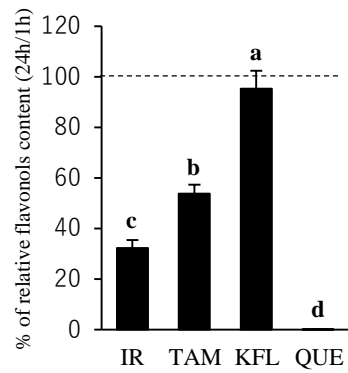
b



c



d



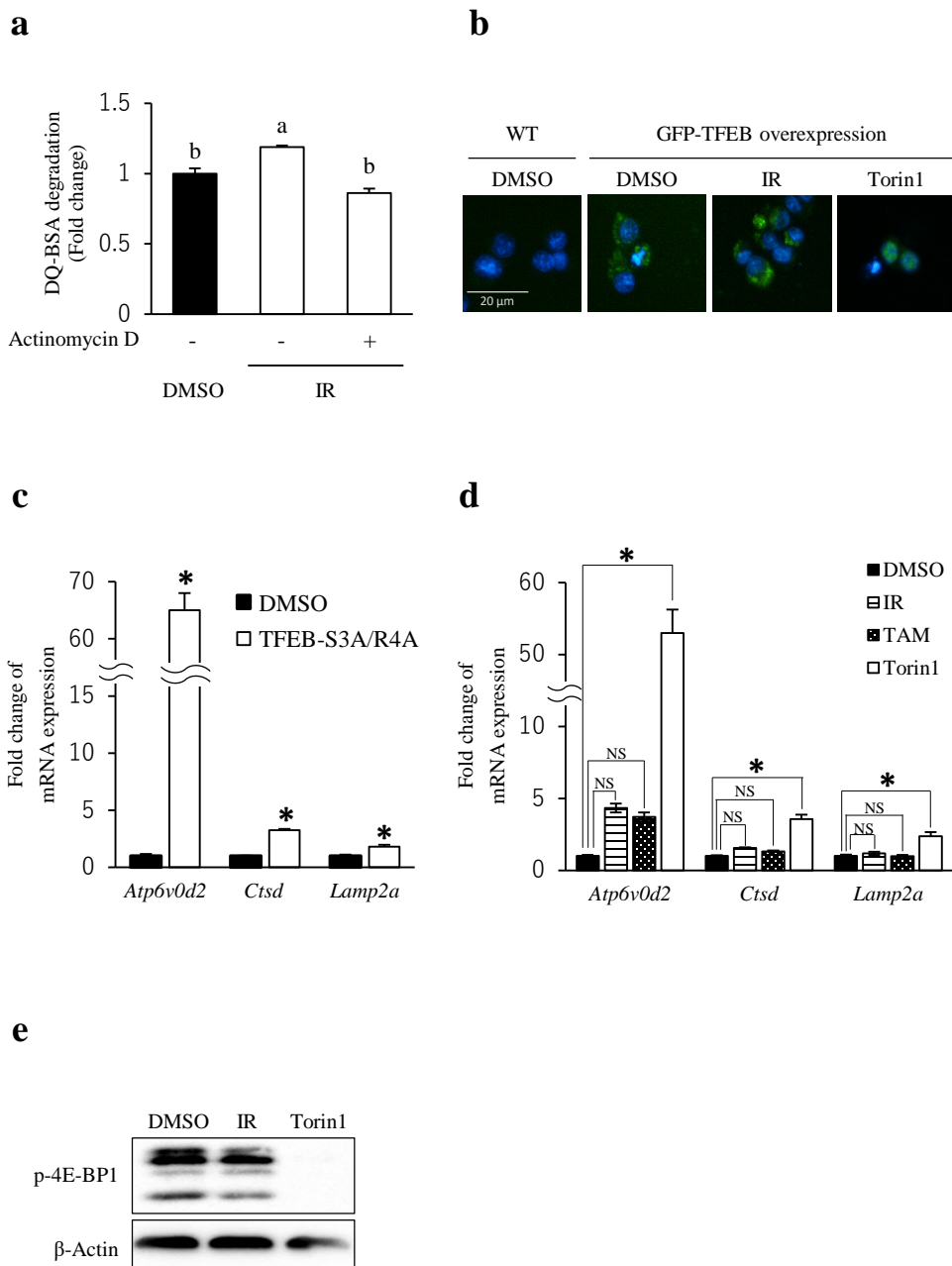


Figure 4, Sakai M *et al.*